New Journal of Chemistry

Electronic Supplementary Materials

Donor–acceptor type polymers containing 2,3-bis(2-pyridyl)-5,8-dibromoquinoxaline acceptor and different thiophenes donors: Electrochemical, spectroelectrochemistry and electrochromic properties

Shuang Chen[1,2], Di Zhang[1,2], Min Wang[2], Lingqian Kong[3], Jinsheng Zhao[2*]

[1]Department of Chemical Engineering, China University of Petroleum (East China), QingDao, 266580, P. R. China

[2]Shandong Key Laboratory of Chemical Energy Storage and Novel Cell Technology, Liaocheng University, Liaocheng, 252059, P. R. China

Corresponding author, Tel: +86-635-8539607; Fax: +86-635-8539607.

E-mail address: j.s.zhao@163.com (j.s.zhao);

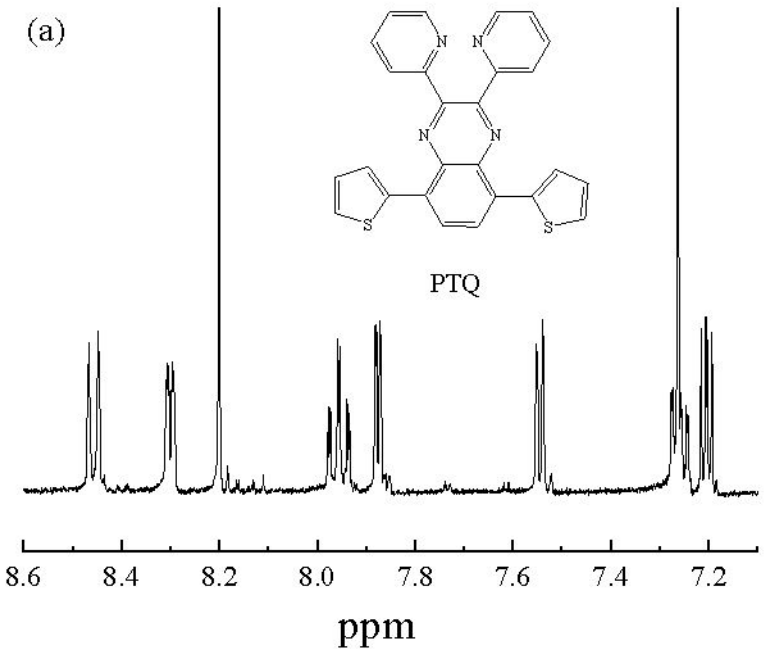
(a)
N
N
N
N
S
S
PTQ
8.6
8.4
8.2
8.0
7.8
7.6
7.4
7.2
ppm

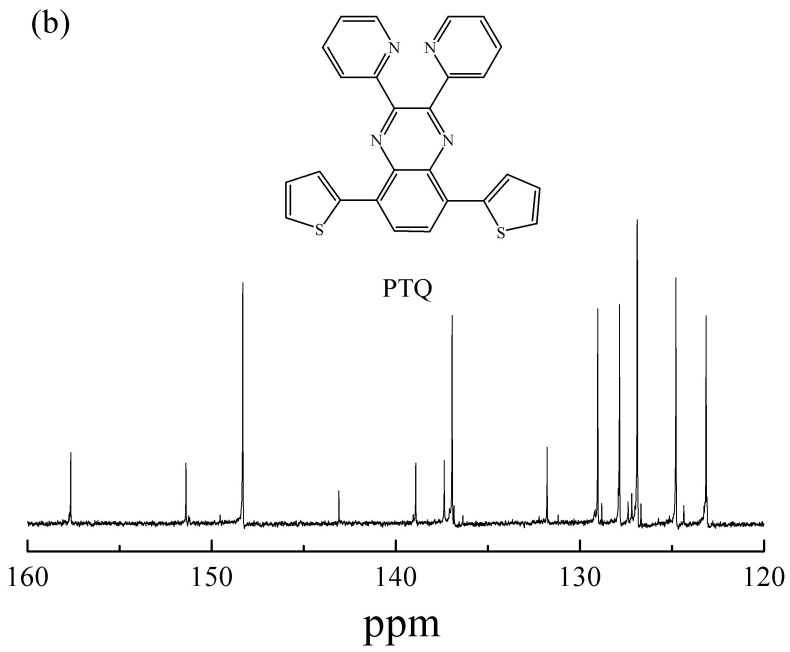

Fig. S1. (a) ^{1}H NMR spectrum of 2,3-di(2-pyridyl)-5,8-bis(2-thienyl) quinoxaline (PTQ) in $CDCl_3$. (b) ^{13}C NMR spectrum of PTQ in $CDCl_3$.

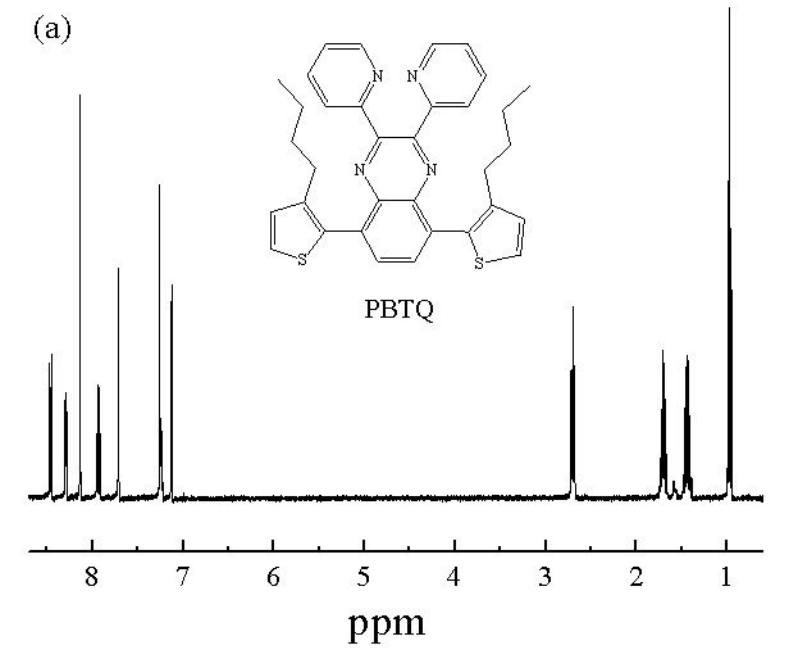

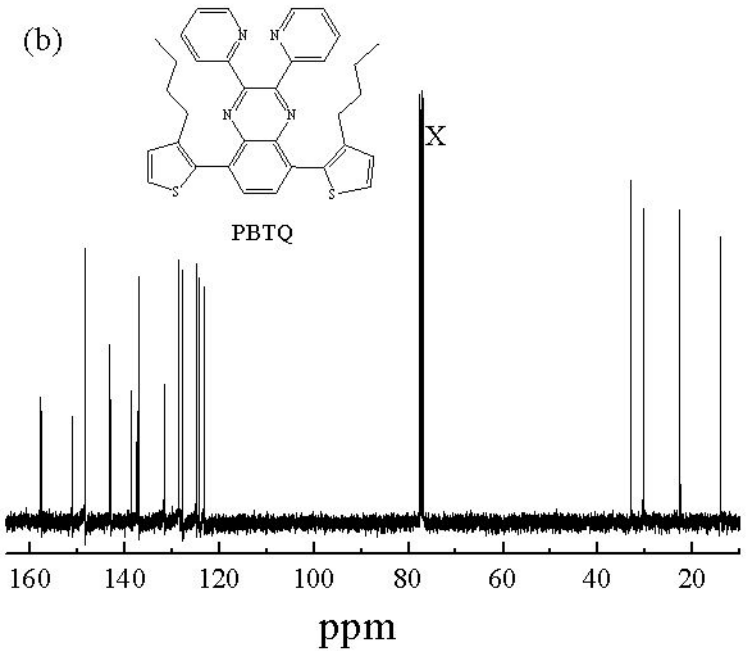

Fig. S2. (a) ^{1}H NMR spectrum of 2,3-di(2-pyridyl)-5,8-bis(3-butylthiophen-2-yl)) quinoxaline (PBTQ) in $CDCl_3$. (b) ^{13}C NMR spectrum of PBTQ in $CDCl_3$. Solvent peak at δ = 77.26 ppm is marked by 'X'.

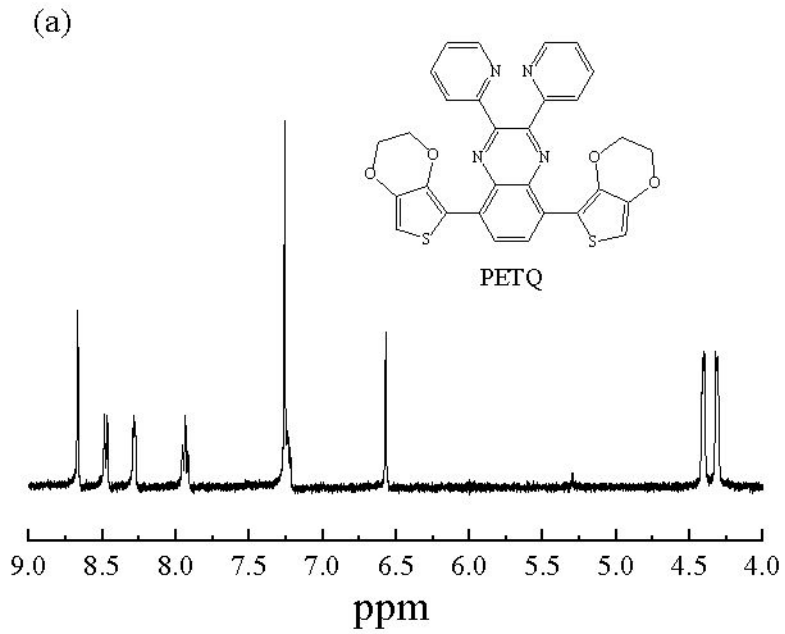

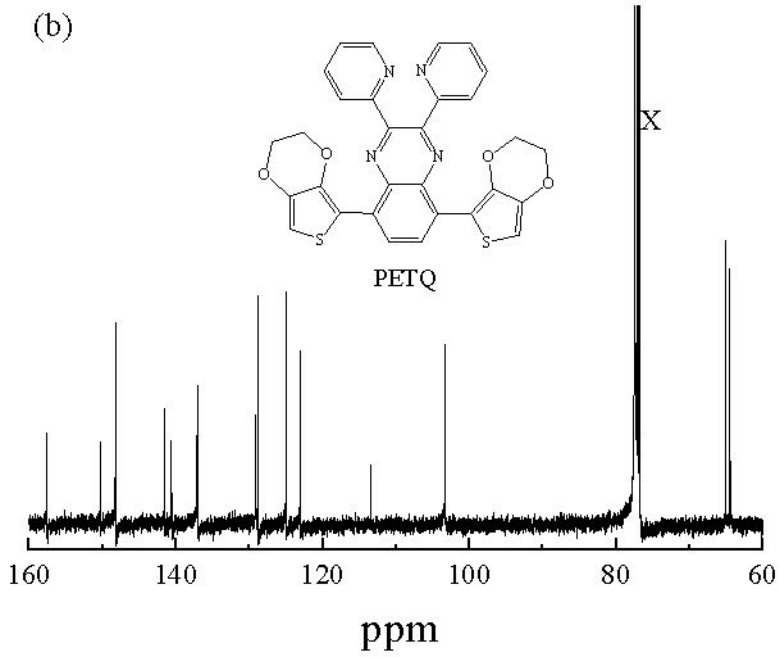

Fig. S3. (a) ^{1}H NMR spectrum of 2,3-di(2-pyridyl)-5,8-bis(2-(3,4-ethylenedioxythienyl)) quinoxaline (PETQ) in $CDCl_3$. (b) ^{13}C NMR spectrum of PETQ in $CDCl_3$. Solvent peak at δ = 77.174 ppm is marked by 'X'.

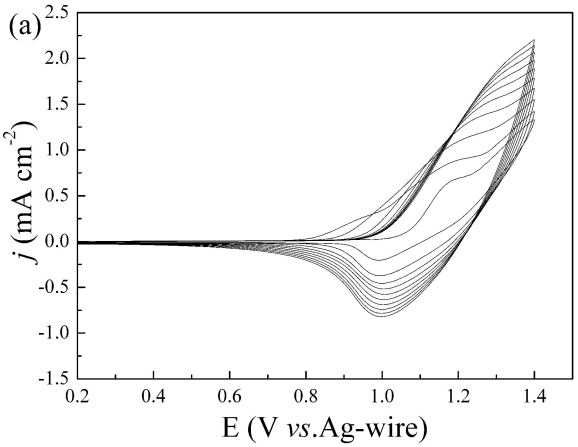

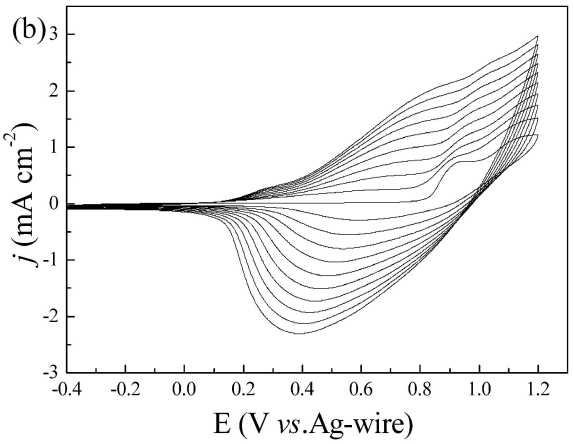

Fig. S4. Cyclic voltammogram curves of PBTQ (a) and PETQ (b) in 0.1 M $TBAPF_6$/ DCM solution at a scan rate of 100 mV s^{-1} respectively. *j* denotes the current density. E denotes the potential.

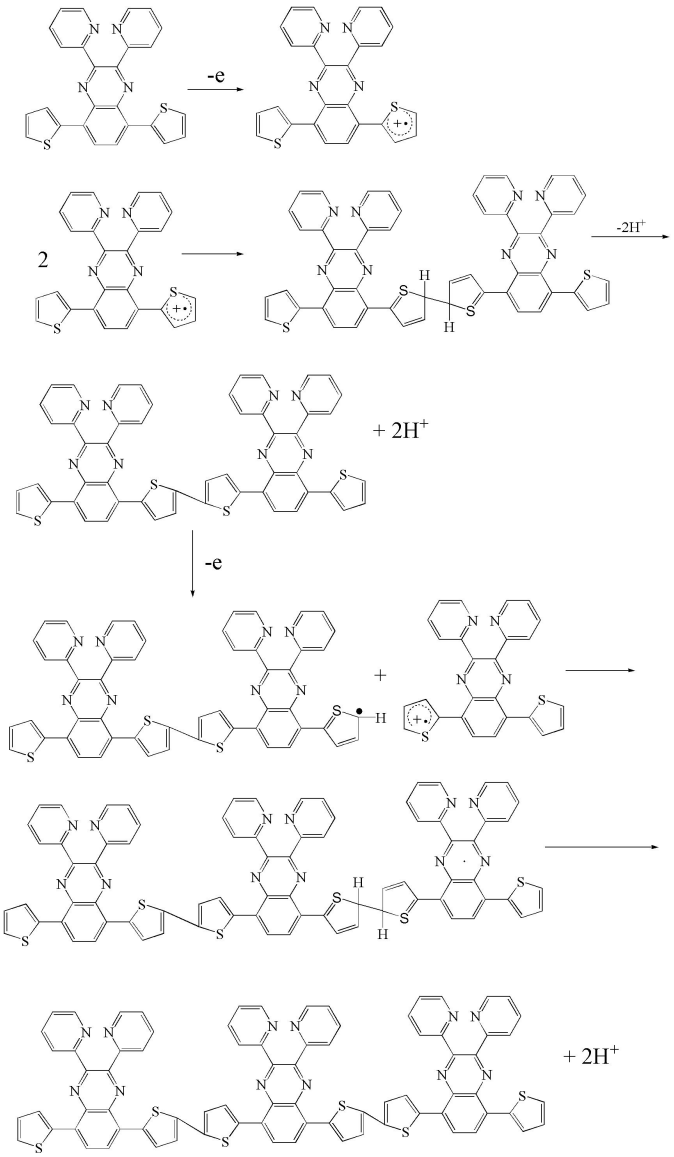

Fig.S5. The electrochemical polymerization mechanism of the syntheis of the polymer PPTQ

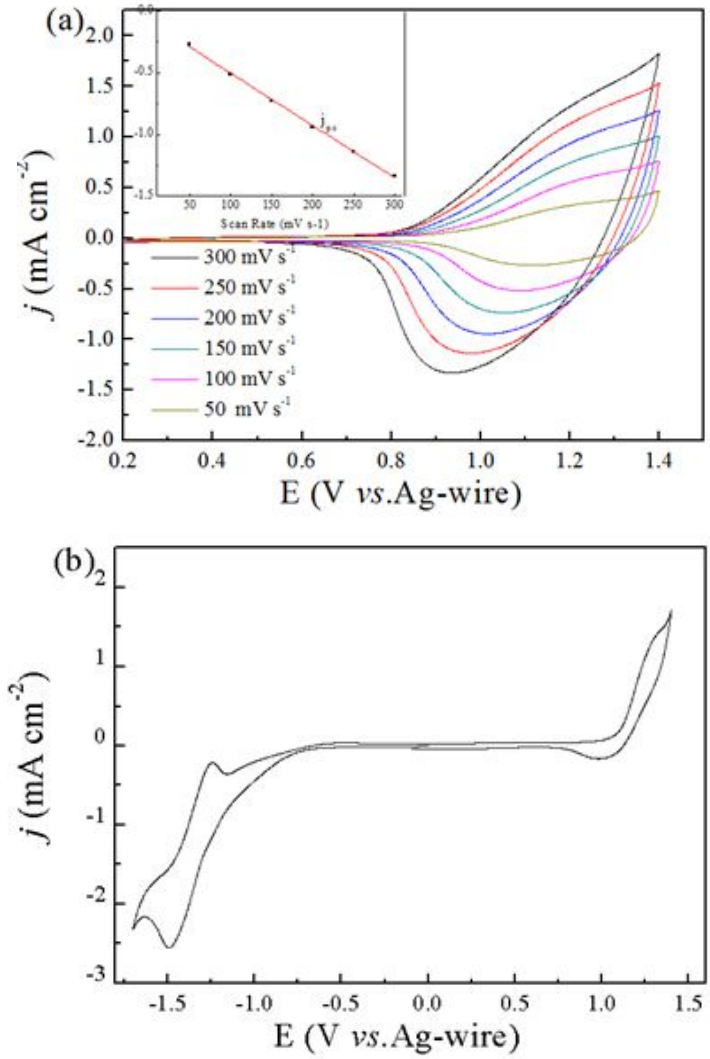

Fig. S6. (a) CV curves of PPTQ at different scan rates between 50 and 300 mV s^{-1} in the monomer-free 0.1 M $TBAPF_6$/DCM solution. Inset shows scan rate dependence of the anodic and cathodic peak current densities graph. $j_{p.c}$ denotes cathodic peak current densities. (b) The cyclic voltammogram of the PTQ monomer at scan rate 100 mV s^{-1}.

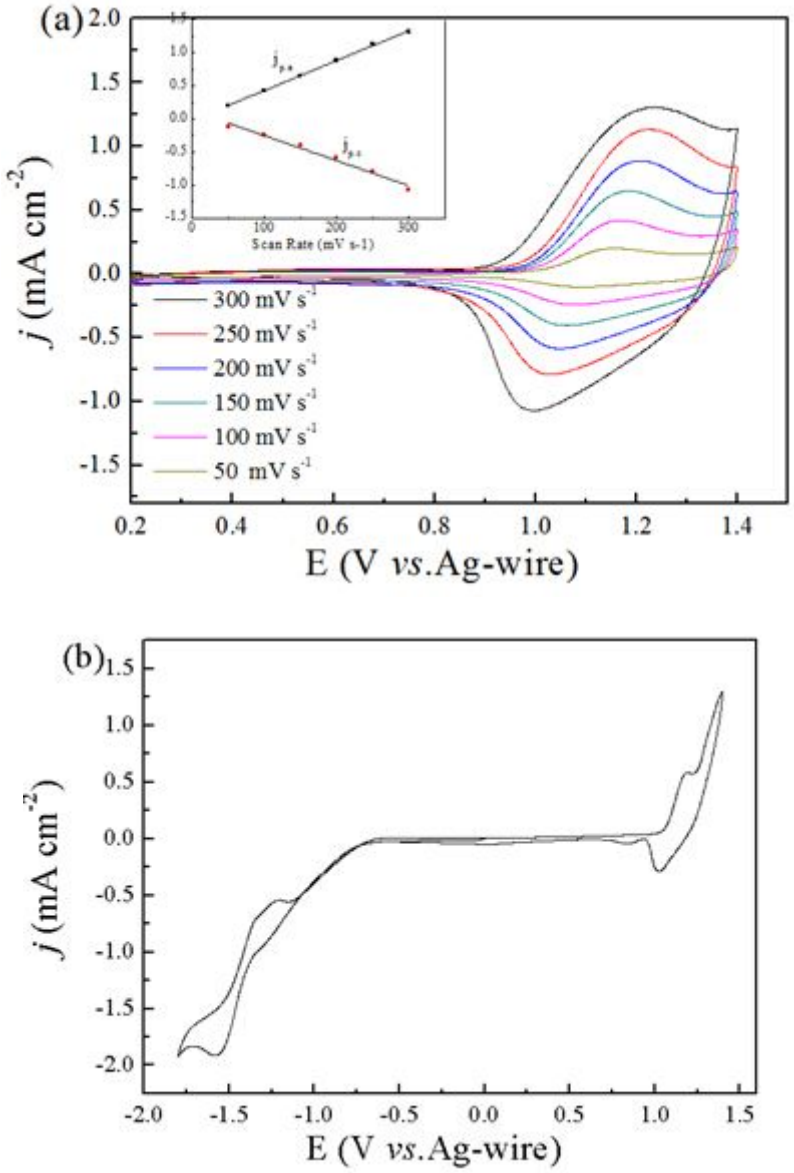

Fig. S7. (a) CV curves of PPBTQ at different scan rates between 50 and 300 mV s^{-1} in the monomer-free 0.1 M $TBAPF_6$/DCM solution. Inset shows scan rate dependence of the anodic and cathodic peak current densities graph. $j_{p.a}$ and $j_{p.c}$ denote the anodic and cathodic peak current densities, respectively. (b) The cyclic voltammogram of the PBTQ monomer at scan rate 100 mV s^{-1}.

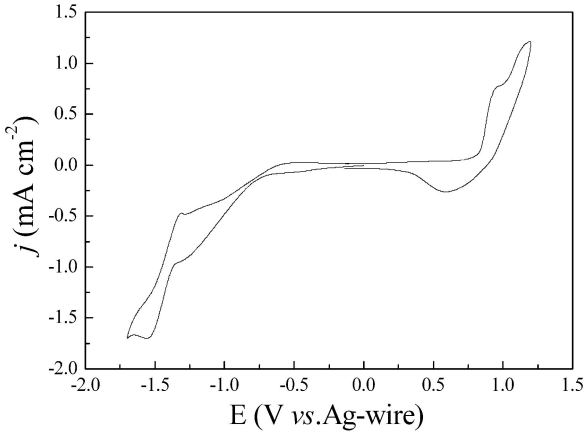

Fig. S8. The cyclic voltammogram of the PETQ monomer at scan rate 100 mV s^{-1}.

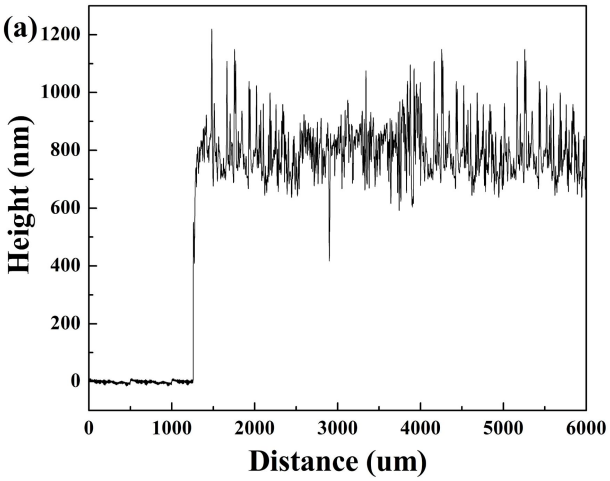

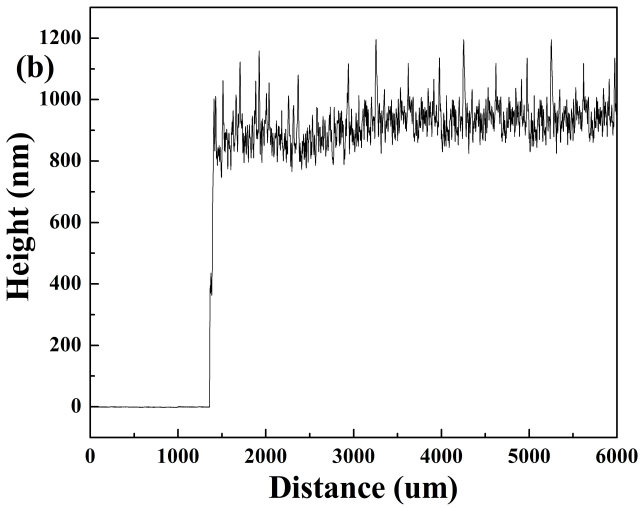

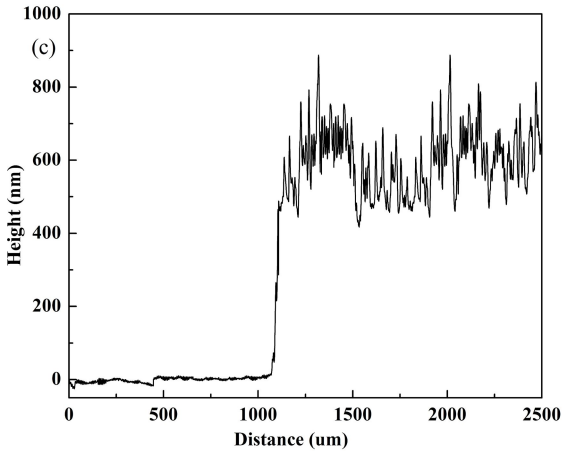

Fig.S9. The step profiler images of PPTQ (a), PPBTQ(b) and PPETQ (c) films deposited potentiostatically on ITO electrode with the same polymerization charge of 2.0×10^{-2} C at a surface area of 0.9×1.8 cm^2.

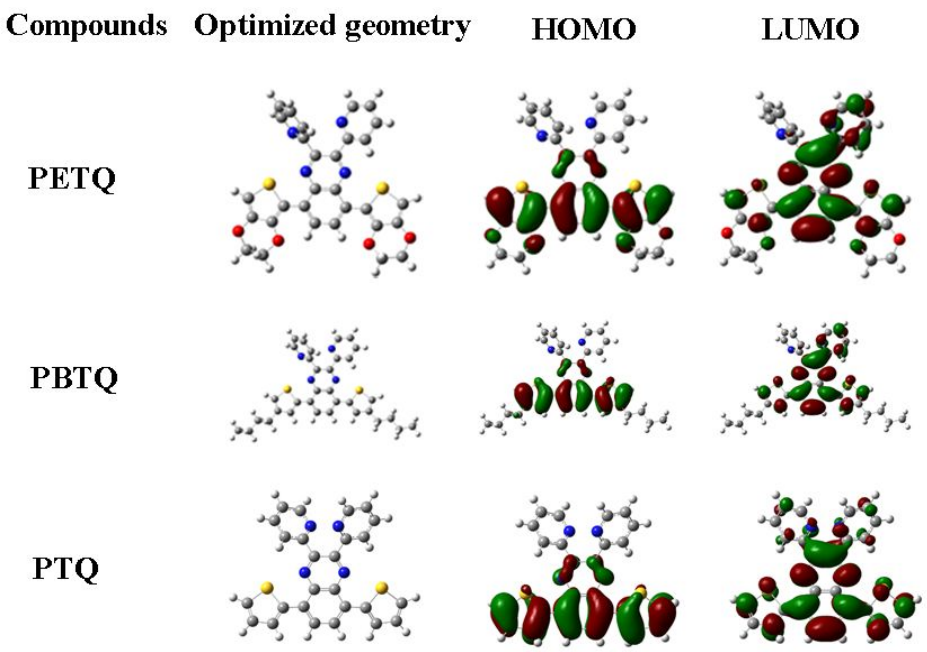

Fig. S10. The optimized geometries and the molecular orbital surfaces of the HOMOs and LUMOs for three monomers.